POLITECNICO DI TORINO
Repository ISTITUZIONALE

Research on the Automobile Aerodynamic Field at the Politecnico di Torino in the Second Half of the Twentieth Century

Original
Research on the Automobile Aerodynamic Field at the Politecnico di Torino in the Second Half of the Twentieth Century / Nuccio, P.. - In: SAE TECHNICAL PAPER. - ISSN 0148-7191. - ELETTRONICO. - 1:(2023). (WCX SAE World Congress Experience Detroit) [10.4271/2023-01-0015].

Availability:
This version is available at: 11583/2978384 since: 2023-05-08T08:18:55Z

Publisher:
SAE

Published
DOI:10.4271/2023-01-0015

Terms of use:

This article is made available under terms and conditions as specified in the corresponding bibliographic description in the repository

Publisher copyright
GENERICO -- per es. EPJ (European Physical Journal) : quando richiesto un rinvio generico specifico per

This is a post-peer-review, pre-copyedit version of an article published in SAE TECHNICAL PAPER. The final authenticated version is available online at: http://dx.doi.org/10.4271/2023-01-0015

(Article begins on next page)

13 June 2026

Cable Detection and Manipulation for DLO-in-Hole Assembly Tasks

Kevin Galassi, Alessio Caporali, Gianluca Palli

***Abstract*—This paper describes a cyber-physical system for the manipulation of Deformable Linear Objects (DLOs) addressing the DLO-in-hole insertion problem targeting an industrial scenario, the switchgear's components cabling task. In particular, the task considered is the insertion of DLOs in the switchgear components' holes. This task is very challenging since a precise knowledge of the DLO tip position and orientation is required for a successful operation. We tackled the DLO-in-hole problem from the computer vision perspective constraining our setup on employing just simple 2D images and by using the mobility of the robotic arm for achieving the full 3D knowledge of the DLOs. Then, the DLO tip is detected from two different image planes and the robot's trajectory corrected accordingly before insertion. To prove the effectiveness of the proposed solution, an example scenario is prepared and the method validated experimentally attempting the insertion of several DLOs in a sample switchgear component, obtaining an overall insertion success rate of 82.5%.**

***Index Terms*—Robotic Manipulation, Deformable Objects, Cyber-Physical System, Industrial Manufacturing.**

I. Introduction

In recent years, the increase of automatic machines and electronic devices has highlighted the problem of the production and the manufacturing of switchgears and cable harnesses, nowadays still subject to human labor. The application of robotics for the manipulation of these objects is indeed very limited, and this condition is shared among all the class Deformable Linear Objects (DLOs), comprising not only cables and harnesses but also ropes, suture threads, wires, etc.

Unsurprisingly, the major adversity when dealing with DLOs is their property of being deformable, meaning that their properties change during the time as consequence of the manipulation. In addition, also the visual perception is challenging due to the limited features that can be exploited for their detection. Another problem to overcome is the environment in which these materials have to be manipulated. As a matter of fact, for the large range of applications where DLOs are involved, the workspace is characterized by narrow spaces and a large presence of obstacles, an example can be the production of control boxes where the cables have to be manipulated inside the control box's ducts.

Kevin Galassi, Alessio Caporali and Gianluca Palli are with DEI - Department of Electrical, Electronic and Information Engineering, University of Bologna, Viale Risorgimento 2, 40136 Bologna, Italy.

This work was supported by the European Commission's Horizon 2020 Framework Programme with the project REMODEL - Robotic technologies for the manipulation of complex deformable linear objects - under grant agreement No 870133.

Corresponding author: *kevin.galassi2@unibo.it*

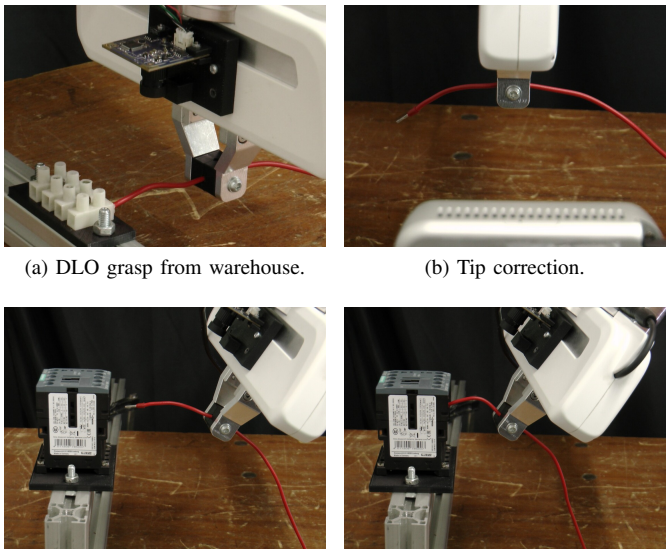

(a) DLO grasp from warehouse. (b) Tip correction. (c) Initial insertion. (d) Insertion completed.

Fig. 1: Snapshots of the insertion task sequence. The robot uses a novel 2D-based shape estimation to locate and grasp the cable (a), then moves the cable to the second camera (b) to perform the correction of the trajectories (c) and allow the insertion (d) of the DLO inside a component of a control panel.

The task of peg insertion, named as peg-in-hole, is a representative robotic task which requires the insertion of an object of a known shape inside an orifice. In the literature, common approaches to this problem are the usage of external force measuring systems placed between the robot and the end-effector link or, as alternative, a compliance-based system [1], to estimate the interaction force between the object and the desired hole. In this scenario, however, the deformability of the material precludes the usage of a force-based interaction. This situation can be viewed as a novel class of problems defined as DLO-in-Hole and new approaches for solving them need to be proposed. Fig. 1 provides an example scenario in which the DLO-in-Hole tasks may find applicability.

Ideally, a precise knowledge of the DLO's tip position and orientation in the workspace needs to be available before performing the insertion. However, DLOs' lack in relevant features and missing characteristics make them hard to be detected and processed by commonly used 3D devices [2] in robotic application. Indeed, DLOs such as the one threaded in this work, consisting of cables and wires of just few millimeters of diameter, are properly perceived only by high-end

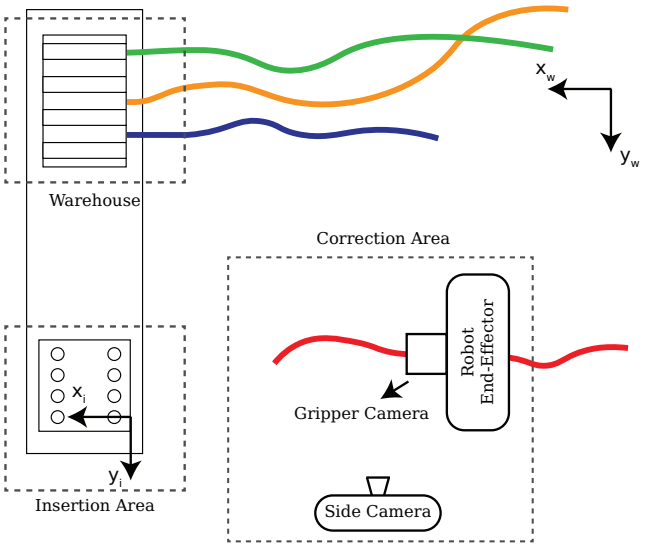

Fig. 2: Experimental Setup. A 2D camera is mounted on the robot end effector to detect and estimate a 3D model of the wire inside the grasp area (Warehouse). The side camera and the gripper camera are used to correct the tip position and orientation after the grasp and before the insertion (Correction Area). The insertion is executed in the Insertion Area.

3D active cameras like Zivid and Photoneo ones [2]. However, such devices are hard to mount on the robot end-effector due to their size, weight and bulkiness. Considering also their intrinsic limitation on the field of view and range, they are usually constrained on fixed setups limiting their applicability. These considerations led to our previous work [3] where we introduced a triangulation-based 3D estimation algorithm that employs the mobility of a robotic arm and a calibrated 2D eye-in-hand camera to achieve the 3D knowledge of the DLO from multiple images.

In this paper, some preliminary results concerning the DLO-in-Hole assembly task are presented. An algorithm called ARIADNE+ [4] is used to detect the DLOs from each input camera image through deep-learning based segmentation and providing a B-Spline representation of the DLO in pixel coordinates. Then, by collecting the estimated 2D splines provided by different points of views, an evolution of the method first presented in [3] estimates the 3D shape of the DLO described by means of a spline in the 3D Cartesian space. The main contribution of this paper is in showing how with just 2D cameras and proper trajectories of the robotic arm it is possible to achieve successful results in the DLO-in-Hole task, starting from the DLO 3D estimation and grasp, its tip point correction and finally insertion.

The paper is organized as follows: in Sec. II the relevant literature related to this problem is presented. Then, the task proposed is presented in Sec. III and explained in details in Secs. IV-V. Finally, in Sec. VI the method is experimentally evaluated and the conclusions are reported in Sec. VII.

II. Related Works

The DLO-in-Hole problem is a relevant research topic that has been studied along the years proposing alternative solutions to this challenging task. In [5] the authors propose to control the trajectories by estimating the shape of the object, in that work the target was a deformable beam which is definitely easier to model and estimate compared to a long wire. Another approach to fulfill the insertion is from estimation of the deformation starting from the study of the potential energy as seen in [6] and using the over mentioned approach in [7] the author use the robot to manually bend the plastic material to shape the cable. A more recent work proposes the usage of tactile sensors mounted on the fingers' tip to estimate the deformability of the wire to permit the insertion in a hollow cylinder [8] or in a control box component [9]. From the opposite perspective, other research aimed at the insertion of rigid object inside a flexible material [10], [11].

From the DLOs perception point of view, although it is an active research topic [12], the detection and segmentation of DLOs has been commonly addressed in simple setting, such as marker-based [13], background color removal [14]–[16], Frangi filter [17], Ridge filter [18] or ELSD algorithm [19]. In [20], the authors proposed an algorithm called ARIADNE where the individual DLOs are segmented from complex backgrounds starting from their endpoints, which are detected by a CNN. Additionally, each segmented DLO is modeled with a B-spline curve to ease further manipulations. The segmentation of DLOs (specifically wires) via learning-based methods has been attempted in [21] where a dataset consisting of electric wires is made publicly available. Instead of vision-based approaches, some works have focused the attention on tactile sensors placed on the fingers of the robot gripper. This approach is better suited in case of occlusions and space limitation, and these sensors can provide important information in manipulation tasks [22]. Additionally, vision and tactile data can also be combined [23] to overcome the limitation of both solutions.

III. Setup and Task Description

The task proposed in this paper consists in the DLO-in-Hole problem, where a DLO needs to be inserted by a robot into an electromechanical component connection socket.

In Fig. 2 the setup used for the experimental evaluation of the approach presented in this paper is shown. The setup reproduces the problem of wire insertion in a know position, for example in the switchgear cabling scenario, simulating the extraction of the cable from a warehouse that collects the wires and the following insertion in a component where a second robot or a human operator can secure the cable by means of a screwdriver. Concerning the sensors, a low-cost 2D camera (ELP-USB8MP02G-L75) camera is placed in an eye-in-hand configuration and calibrated both intrinsically and extrinsically. This camera is addressed in the following as *gripper camera* and it is shown also in Fig. 1a on the robot end-effector. The *gripper camera* is calibrated utilizing, for the extrinsic parameters, an initial guess obtained from

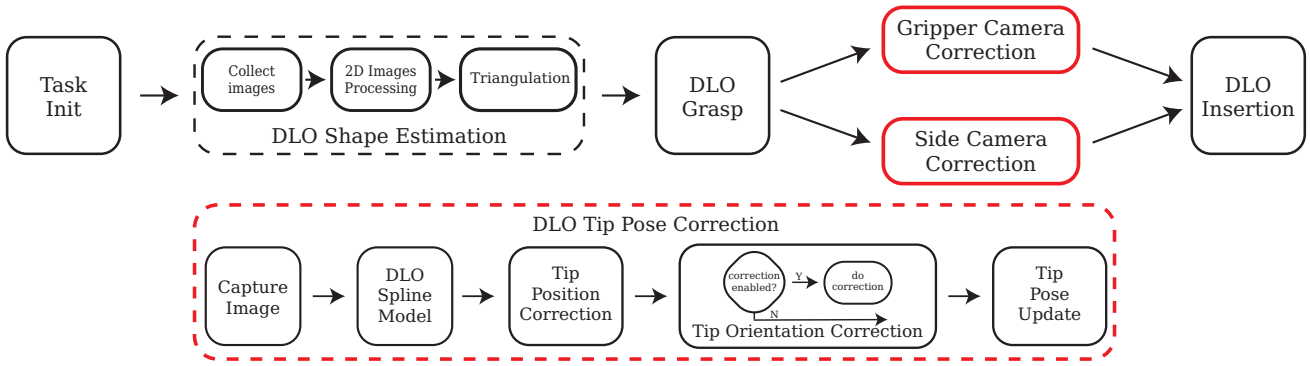

Fig. 3: System execution pipeline. The robot estimates the precise DLO shape using multiple images collected from a 2D camera. After, the grasping is performed. From the images coming from the *gripper camera* and a fixed second *side camera* the correction of the tip pose is performed. The sequence is terminated with the DLO insertion. The correction of the orientation can be enabled or disabled (more in the experimental section), thus the if condition.

the CAD files which is then further refined by using an eye-in-hand calibration algorithm employing a chessboard pattern [24], [25]. In addition, a second camera (RealSense D435) is placed in the designated *correction* area, and in the reminder of the paper it is addressed as *side camera*, shown also in Fig. 1b. This camera is not calibrated extrinsically with the robot, instead is taken advantage of the knowledge of the 3D model of the DLO to convert pixel coordinate into an estimate in world coordinates. As a remark, the selection of the *side camera* is due only to internal availability as only the RGB image (not the Depth) is used in this work.

The DLO-in-Hole task is challenging mostly due to the deformability of the object being manipulated, hence the need to estimate the tip pose precisely before the insertion. To tackle these challenges, in this work is proposed a strategy schematized in Fig. 3. The task begins with the robot moving to the warehouse area where the DLO(s) are stored. After selecting the target DLO, the robot performs the acquisition of several images with the *gripper camera* which are then processed obtaining a 3D model of the DLO represented as a sequence of 3D cartesian points interpolated by a spline curve. Details of this process are provided in Sec. IV. Obtained the full 3D knowledge of the DLO, the robot performs the DLO grasp at a pose with a specific distance (specified by the user) from the detected tip. Now the robot moves to the area designed for the correction procedure, where the intrinsic deformability of the DLO and the possible additional deformations that occurred during the grasp and extraction from the warehouse are taken into account. In particular, the position offset between the gripper fingers frame and the DLO tip is computed. Additionally, also the orientation of the DLO tip is estimated and the gripper rotated accordingly to align the DLO's tip direction with the known hole frame. The tip correction is executed employing both the *gripper camera* and *side camera*. Details on these two correction procedures are provided in Sec. V. Finally, the robot moves toward the target hole and performs the insertion, where the precise location of the hole is assumed to be known.

IV. DLO Shape Estimation

In this section is provided the details about the DLO shape estimation procedure mentioned in Fig. 3. In particular, we mostly followed the approach firstly presented in [3], that we briefly summarized here.

A. 2D Image Processing

Concerning the 2D image processing, we adopt a deep convolution neural network (DeepLabV3+ [26]) for the background segmentation. The network is trained on a synthetic dataset [21] built utilizing a chroma-key based approach which allows a generation of a large amount of data with minimum human effort. The dataset features both complex cluttered backgrounds and more simple ones, aiming at a complete generalization in all the possible scenarios, including the industrial one. Given the binary mask of the image, in which background pixels (black) are separated from the foreground ones (white), a superpixel segmentation is applied on the latter. The idea of superpixels is to partition the image into local meaningful areas making the further processing easier and faster. In particular, we deploy MaskSlic [27], a modified version of the more famous Simple Linear Iterative Clustering (SLIC) [28] algorithm, which uses color and proximity pixel information in a 5D space for the segmentation only on a region of interest (i.e. the foreground pixels). Based on the superpixel label map, a region adjacency graph (RAG) is built. That is, an undirected and unweighted graph where each superpixel is represented as a graph node and the edges are computed from neighbouring relationships between superpixels. Concerning the cables' terminals detection, they can be extracted simply from the graph as the nodes characterized by having only one neighbor. Finally, fast *walks* are performed on the graph aiming at organizing the set of graph nodes as an ordered sequence from one terminal to another of the DLO considered. Finally, the obtained *walk* is used to estimate a 2D spline representing the DLO in the current image plane, as:

$$q(u) = \sum_{i=1}^{n_u} b_i(u) q_i \tag{1}$$

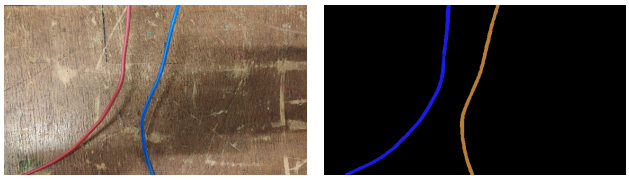

(a) Source image (b) Output colored mask

Fig. 4: Example of image processing. The two DLOs are segmented from the input image into individual instances (denoted by different color in the output mask).

where u is a free coordinate representing the position along the DLO starting from an endpoint ($u = 0$) to the opposite ($u = L$, being L the length of the DLO), $q(u) = [p_x(u)\ p_y(u)]^T$ is the 2D vector of pixel coordinates representing the estimated spline in the input image, $b_i(u)$ is the i-th elements of the spline polynomial basis used to represent the DLO shape and q_i are n_u properly selected coefficients, usually called *control points*, used to interpolate the DLO shape through the $b_i(u)$ function basis.

B. 3D Shape Estimation

To asses the 3D knowledge of the DLO, multiple image samples are collected from different view points. In particular, the robot end-effector equipped with the *gripper camera* is used to mimic a stereo device. Thus, a trajectory is specified and parameterized with a user-defined number of poses for the acquisition of sample images with a known baseline, following the standard normal stereo setup. For each acquired image, the detection pipeline described in Sec. IV-A is applied and the computed spline of the frame under exam is stored together with the relative pose of the camera. Then, the set of splines is triangulated point-wise in order to estimate the 3D shape of the DLO considered. In details, given a generic point in the cartesian space x, and provided that n_p distinguished points of view are available, the estimation $\tilde{x}$ of the unknown point x can be obtained by looking for the point having the minimum distance from all the rays v_i. By defining the symmetric V_i matrix

$$V_i = I - {}^w v_i {}^w v_i^T \tag{2}$$

providing the seminorm on the ray distance, the point location estimate $\tilde{x}$ is provided by nearest point search algorithm, i.e.

$$\tilde{x} = \left(\sum_{i=1}^{n_p} V_i \right)^{-1} \left(\sum_{i=1}^{n_p} V_i {}^w t_{c_i} \right) \tag{3}$$

where ${}^w t_{c_i}$ is the position of the camera frame origin in world coordinates and ${}^w v_i$ is the unit ray in world coordinates passing through the image reference frame origin and x expressed as function of pixel coordinates p_i of x and the camera focal distance f.

The aforementioned approach is carried out on a suitable set of sample point along the DLO spline. Let us call the set of spline samples $p_{ij} = p_i(u_j)$, $j = 1, \dots, n_s$, $i = 1, \dots, n_p$, where n_s is the number of spline samples, n_p is the number of points of view, $p_i(\cdot)$ is the spline provided for by the i-th image and u_j are the spline sample points.

The vector of control points $q_v = [q_1 \ \cdots \ q_{n_u}]^T$ of the 3D spline $q(u)$ that optimally approximated the set of point estimates p_{ij} can be defined as

$$q_v = B^{\#} \tilde{x}_v \tag{4}$$

where $^{\#}$ represents the matrix pseudoinverse and

$$B = \begin{bmatrix} b_1(u_1) & \cdots & b_{n_u}(u_1) \\ b_1(u_2) & \cdots & b_{n_u}(u_2) \\ \vdots & \vdots & \vdots \\ b_1(u_{n_s}) & \cdots & b_{n_u}(u_{n_s}) \end{bmatrix}$$

$$\tilde{x}_v = \begin{bmatrix} \left(\sum_{i=1}^{n_p} V_{i1}\right)^{-1} \left(\sum_{i=1}^{n_p} V_{i1} {}^w t_{c_i}\right) \\ \left(\sum_{i=1}^{n_p} V_{i2}\right)^{-1} \left(\sum_{i=1}^{n_p} V_{i2} {}^w t_{c_i}\right) \\ \vdots \\ \left(\sum_{i=1}^{n_p} V_{in_s}\right)^{-1} \left(\sum_{i=1}^{n_p} V_{in_s} {}^w t_{c_i}\right) \end{bmatrix}$$

being V_{ij} the matrix computed according to eq. (2) for the j-th sample provided by the i-th image.

V. DLO Tip Correction and Trajectory Planning

Once the gripper has completed the grasp operation, the DLO is extracted from the warehouse and brought to a predetermined area, namely *correction area*, where both the corrections employing the *gripper camera* and *side camera* are performed. Notice that the target pose $P_{correction}$ for the gripper is chosen such that the DLO of interest is completely observable from the 2D camera placed externally.

Let's focus on the correction performed by the *gripper camera* which main idea is schematized in Fig. 5. This correction is performed on a plane parallel to the xy world plane, thus the gripper axis z_g is assumed to be aligned with the world axis z_w. A sample image is captured and the current spline model of the grasped DLO obtained via Sec. IV-A. The tip of the DLO is selected as the endpoint having the minimum row pixel value. This is a reasonable assumption since the DLO is assumed to be grasped. The tangent of the spline at the tip point is evaluated and in this way the tip direction established. The tip position described in pixel coordinates is then converted in cartesian coordinates in the gripper frame assuming a fixed depth of the DLO form the camera, i.e. as the static distance between the camera and gripper frames, and the quantities x_t and y_t are thus obtained. The offset along the x_g and y_g axes are then easily computed as d_x and d_y respectively, see Fig. 5a, and used to correct the target frame used during the insertion. Additionally, the direction information can be used to rotate the gripper around the z_g axis and align the DLO tip to the hole approaching direction, as shown in Fig. 5b.

Considering instead the correction performed by the *side camera*, the procedure followed is similar to what already described for the *gripper camera*. The main difference is that this time the camera is not calibrated. This choice was made to alleviate the constrains on the setup and evaluate the effectiveness of the approach with this additional constraint.

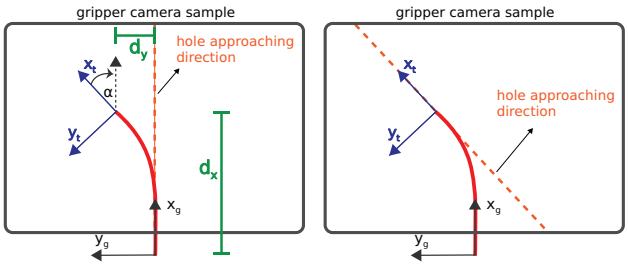

(a) Initial Condition (b) Correction

Fig. 5: Gripper camera correction.

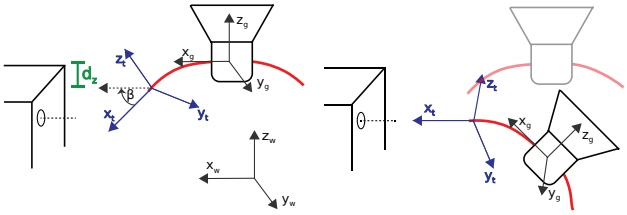

(a) Initial Condition (b) Correction

Fig. 6: Side camera correction.

However, the approach can be easily modified to accommodate a full calibrated setup and comparisons with that scenario are going to be established as future research. The *side camera* is used to perform a correction on the along the z_w axis, since this was not achievable with the *gripper camera* With reference to Fig. 6, the DLO tip is now obtained as the DLO having the minimum column value in the image. The tip position in the gripper frame is obtained by scaling the pixel values knowing the length of the DLO between the gripper frame and its tip. This knowledge comes from the moment of the grasp where the grasp pose is parametrized to the detected DLO length from its 3D estimated model. Like before, the offset d_z between z_g and z_t is computed and used to correct the last component of the target frame used during the insertion. Additionally, the direction of the DLO tip computed via the spline tangent can be used to correct also the target frame orientation, as shown in Fig. 6b.

Overall, the target frame for the insertion is obtained starting from the gripper frame as:

$$\begin{bmatrix} X \\ Y \\ Z \end{bmatrix} = \begin{bmatrix} x_g \\ y_g \\ z_g \end{bmatrix} + \begin{bmatrix} d_x \\ d_y \\ d_z \end{bmatrix} \tag{5}$$

When the orientation correction is considered, the robot rotates around the tip to align the cable along the insertion direction. the final direction of the gripper can be obtained as:

$$R'_g = R_g \, R_z(\alpha) R_y(\beta) \tag{6}$$

where $R_z(\alpha)$ and $R_y(\beta)$ are the rotation matrix obtained using the two correction angles obtained respectively from the *gripper camera* and the *side camera*.

VI. Experimental Evaluation

To validate the proposed approach, a series of insertions of electrical wires in an electromechanical component connection socket have been performed. The wires have a diameter of 2 mm wheres the hole diameter is 5 mm. It is important to remark that the challenge in this experiment, apart from the DLO deformability and difficulty in the detection in a vision-based system, resides in the presence of a screw inside the hole that it is used to secure the connection and that could make the DLO tip change orientation in case of contact. To make the experiment resemble more closely a possible application for a switchgear cabling system, after the insertion of the wire, a human operator secures the wire using a screwdriver. Then, the robot pulls away from the hole. The connection is marked as successful if the wire remains attached to the component after this pull test. We separately tested the case in which we perform only a correction in position or both a correction in position and orientation of the DLO tip. The results after 20 insertions for each case are the following: 17/20 successful insertion in the position only case; 16/20 successful insertion in the position plus orientation case.

These results are not surprising. In fact, we observed that our vision algorithm wasn't always capable of capturing the tip location area in the image with enough accuracy, in particular for what concerns the estimation of the tip direction. Indeed, in the failure cases, the orientation is erroneous leading to a wrong approaching to the hole with the wire tip colliding with the hole contour and blocking its insertion. On the contrary, possible small errors in the estimation of the tip position in the image are less harmful from the point of view of the overall success in the insertion. By pulling the wire after it has been secured and by measuring the external force acting on the gripper, it is possible to identify if the wire has been properly secured and inserted, the result in Fig. 7 offers a clear view of how the two forces are different in magnitude and easily separable. As final note, we would like to remark that, when provided with a reliable orientation estimate, the insertion operation with the correction in orientation enabled

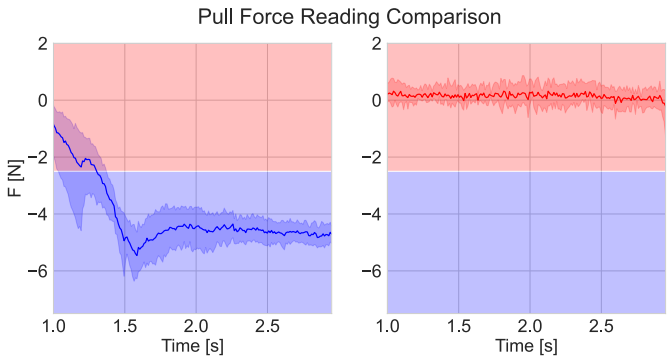

Fig. 7: Comparison of the end-effector force measurements along the pull direction, on the left (blue) the case where the cable is properly connected to the desired components, on the right (red) the case of failed connections.

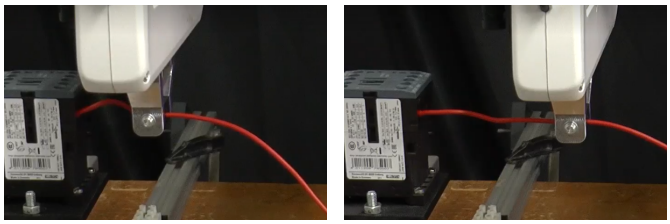

(a) Initial pull condition (b) After pull and sliding

Fig. 8: Snapshots of a pull experiment.

would result into a smoother insertion with limited or absent "jumps" due to undesired tip contacts.

VII. Conclusion

In this paper, a vision-based approach for the execution of DLO-in-Hole insertion tasks has been evaluated. In the proposed solution, a calibrated gripper camera is exploited to obtain first the full 3D knowledge of a DLO and then it is used, in conjunction of a side camera, for correcting the tip position and orientation after the grasp, aiming at a successful insertion in a designated hole. The experiments performed provide useful insight and results, that will be investigated in future research. The experiments also dispense evidence of the misalignment problem between the gripper frame and the DLO, in case of poor grasp operation. This misalignment is currently not recoverable in our setup. In the future, the integration of tactile data in the pipeline will be investigated to account for these errors. Additionally, tactile data can also be employed for detecting the sliding of the DLO between the gripper fingers.

References

[1] H. Park, J. Park, D.-H. Lee, J.-H. Park, M.-H. Baeg, and J.-H. Bae, "Compliance-based robotic peg-in-hole assembly strategy without force feedback," *IEEE Transactions on Industrial Electronics*, vol. 64, no. 8, pp. 6299–6309, 2017.

[2] K. P. Cop, A. Peters, B. L. Žagar, D. Hettegger, and A. C. Knoll, "New metrics for industrial depth sensors evaluation for precise robotic applications," in *Proc. IEEE/RSJ Int. Conf. on Intelligent Robots and Systems*, 2021.

[3] A. Caporali, K. Galassi, and G. Palli, "3d dlo shape detection and grasp planning from multiple 2d views," in *2021 IEEE/ASME International Conference on Advanced Intelligent Mechatronics (AIM)*. IEEE, 2021.

[4] A. Caporali, R. Zanella, D. De Gregorio, and G. Palli, "Ariadne+: Deep learning-based augmented framework for the instance segmentation of wires," *IEEE Transactions on Industrial Informatics*, 2022.

[5] Y. Zheng, R. Pei, and C. Chen, "Strategies for automatic assembly of deformable objects," in *Proceedings. 1991 IEEE International Conference on Robotics and Automation*, 1991, pp. 2598–2603 vol.3.

[6] H. Wakamatsu, S. Hirai, and K. Iwata, "Modeling of linear objects considering bend, twist, and extensional deformations," in *Proceedings of 1995 IEEE International Conference on Robotics and Automation*, vol. 1, 1995, pp. 433–438 vol.1.

[7] H. Nakagaki, K. Kitagi, T. Ogasawara, and H. Tsukune, "Study of insertion task of a flexible wire into a hole by using visual tracking observed by stereo vision," in *Proceedings of IEEE International Conference on Robotics and Automation*, vol. 4, 1996, pp. 3209–3214 vol.4.

[8] R. Zanella, D. De Gregorio, S. Pirozzi, and G. Palli, "Dlo-in-hole for assembly tasks with tactile feedback and lstm networks," in *2019 6th Int. Conference on Control, Decision and Information Technologies (CoDIT)*. IEEE, 2019, pp. 285–290.

[9] D. De Gregorio, R. Zanella, G. Palli, S. Pirozzi, and C. Melchiorri, "Integration of robotic vision and tactile sensing for wire-terminal insertion tasks," *IEEE Tran. on Automation Science and Engineering*, vol. 16, no. 2, pp. 585–598, 2018.

[10] Y. Adagolodjo, L. Goffin, M. De Mathelin, and H. Courtecuisse, "Robotic insertion of flexible needle in deformable structures using inverse finite-element simulation," *IEEE Transactions on Robotics*, vol. 35, no. 3, pp. 697–708, 2019.

[11] W. Edwards, G. Tang, Y. Tian, M. Draelos, J. Izatt, A. Kuo, and K. Hauser, "Data-driven modelling and control for robot needle insertion in deep anterior lamellar keratoplasty," *IEEE Robotics and Automation Letters*, vol. 7, no. 2, pp. 1526–1533, 2022.

[12] J. Sanchez, J.-A. Corrales, B.-C. Bouzgarrou, and Y. Mezouar, "Robotic manipulation and sensing of deformable objects in domestic and industrial applications: a survey," *The Int. Journal of Robotics Research*, vol. 37, no. 7, pp. 688–716, 2018.

[13] X. Jiang, K.-m. Koo, K. Kikuchi, A. Konno, and M. Uchiyama, "Robotized assembly of a wire harness in a car production line," *Advanced Robotics*, vol. 25, no. 3-4, pp. 473–489, 2011.

[14] D. B. Camarillo, K. E. Loewke, C. R. Carlson, and J. K. Salisbury, "Vision based 3-d shape sensing of flexible manipulators," in *Proc. of the ICRA*, 2008, pp. 2940–2947.

[15] T. Tang, C. Wang, and M. Tomizuka, "A framework for manipulating deformable linear objects by coherent point drift," *IEEE Robotics and Automation Letters*, vol. 3, no. 4, pp. 3426–3433, 2018.

[16] M. Yan, Y. Zhu, N. Jin, and J. Bohg, "Self-supervised learning of state estimation for manipulating deformable linear objects," *IEEE Robotics and Automation Letters*, vol. 5, no. 2, pp. 2372–2379, 2020.

[17] A. F. Frangi, W. J. Niessen, K. L. Vincken, and M. A. Viergever, "Multiscale vessel enhancement filtering," in *MICCAI 1998*.

[18] J. Staal, M. D. Abràmoff, M. Niemeijer, M. A. Viergever, and B. Van Ginneken, "Ridge-based vessel segmentation in color images of the retina," *IEEE Tran. on Medical Imaging*, pp. 501–509, 2004.

[19] V. Pătrăucean, P. Gurdjos, and R. G. Von Gioi, "A parameterless line segment and elliptical arc detector with enhanced ellipse fitting," in *ECCV 2012*, pp. 572–585.

[20] D. De Gregorio, G. Palli, and L. Di Stefano, "Let's take a walk on superpixels graphs: Deformable linear objects segmentation and model estimation," in *Lecture Notes in Computer Science - Asian Conference on Computer Vision*. Springer, 2018, pp. 662–677.

[21] R. Zanella, A. Caporali, K. Tadaka, D. De Gregorio, and G. Palli, "Auto-generated wires dataset for semantic segmentation with domain-independence," in *Proc. IEEE Int. Conf. on Computer, Control and Robotics*, 2021, pp. 292–298.

[22] K. Galassi and G. Palli, "Robotic wires manipulation for switchgear cabling and wiring harness manufacturing," in *Proc. IEEE Int. Conf. on Industrial Cyber-Physical Systems*, 2021.

[23] A. Caporali, K. Galassi, G. Laudante, G. Palli, and S. Pirozzi, "Combining vision and tactile data for cable grasping," in *2021 IEEE/ASME International Conference on Advanced Intelligent Mechatronics (AIM)*. IEEE, 2021.

[24] A. Tabb and K. M. Ahmad Yousef, "Solving the robot-world hand-eye(s) calibration problem with iterative methods," *Machine Vision and Applications*, vol. 28, no. 5-6, 2017.

[25] B. Triggs, P. F. McLauchlan, R. I. Hartley, and A. W. Fitzgibbon, "Bundle adjustment—a modern synthesis," in *International workshop on vision algorithms*. Springer, 1999, pp. 298–372.

[26] L.-C. Chen, Y. Zhu, G. Papandreou, F. Schroff, and H. Adam, "Encoder-decoder with atrous separable convolution for semantic image segmentation," in *Proceedings of the European conference on computer vision (ECCV)*, 2018, pp. 801–818.

[27] B. Irving, "maskslic: regional superpixel generation with application to local pathology characterisation in medical images," *arXiv preprint arXiv:1606.09518*, 2016.

[28] R. Achanta, A. Shaji, K. Smith, A. Lucchi, P. Fua, and S. Süsstrunk, "Slic superpixels compared to state-of-the-art superpixel methods," *IEEE transactions on pattern analysis and machine intelligence*, 2012.